Journal of Computational Neuroscience 16, 5–13, 2004

Dendritic I_h Selectively Blocks Temporal Summation of Unsynchronized Distal Inputs in CA1 Pyramidal Neurons

M. MIGLIORE
Department of Neurobiology, Yale University School of Medicine, New Haven, CT, USA; Institute of Biophysics, National Research Council, Palermo, Italy
migliore@spine.med.yale.edu

L. MESSINEO AND M. FERRANTE
Department of Psychology, University of Palermo, Palermo, Italy; Institute of Biophysics, National Research Council, Palermo, Italy

Received May 5, 2003; Revised September 8, 2003; Accepted September 9, 2003

Action Editor: Alain Destexhe

Abstract. The active dendritic conductances shape the input-output properties of many principal neurons in different brain regions, and the various ways in which they regulate neuronal excitability need to be investigated to better understand their functional consequences. Using a realistic model of a hippocampal CA1 pyramidal neuron, we show a major role for the hyperpolarization-activated current, I_h, in regulating the spike probability of a neuron when independent synaptic inputs are activated with different degrees of synchronization and at different distances from the soma. The results allowed us to make the experimentally testable prediction that the I_h in these neurons is needed to reduce neuronal excitability selectively for distal unsynchronized, but not for synchronized, inputs.

Keywords: dendritic integration, I_h, CA1, modeling

Introduction

The rules and the reasons for which neurons develop a specific distribution of dendritic channels are currently under intense experimental and theoretical investigation (reviewed in Migliore and Shepherd, 2002). This interest is related to the paramount importance that the active properties of the dendritic membrane have in defining if, how, and when, action potentials should be generated in response to synaptic inputs. Although most of the background synaptic activity in pyramidal neurons *in vivo* is caused by the unsynchronized activation of synapses over the entire neuron (Destexhe and Pare, 1999; Ho and Destexhe, 2000), there is more and more experimental evidence suggesting an important role for synchronized signals in virtually every higher brain function (Penny et al., 2002).

In the present study, we were interested in elucidating the possible mechanisms allowing a neuron to discriminate (i.e. selectively generate an action potential) between inputs that are synchronous, and therefore likely to be functionally significant, and those that are asynchronous, likely to be of no functional significance. In neocortical and hippocampal CA1 pyramidal neurons, the non-specific, hyperpolarization-activated, cation current I_h, might be specifically involved in this process, because the voltage-dependence and time constant of its activation curve and its non-uniform dendritic distribution (Magee, 1998) seem to be particularly suited to affect EPSPs. In fact, it has

been experimentally shown that the I_h reduces the temporal summation, and normalizes the time course of EPSPs generated at different distances from soma (Magee, 1999; Williams and Stuart, 2000). Thus, given its role as one of the main conductances acting on subthreshold inputs, we have hypothesized that the I_h would differentially affect the temporal integration (and then the probability to elicit a spike) of synchronous or asynchronous synaptic inputs (i.e. activated within a short or long temporal window, with respect to the fast activation of the excitatory receptors). Experimental studies have not yet addressed this important issue. In this paper, we make experimentally testable predictions on how the dendritic I_h may affect the spike probability of a CA1 neuron receiving synaptic inputs activated with different degrees of synchronization at different distances from the soma.

Methods

All the simulations were carried out with the NEURON simulation program (v5.4, Hines and Carnevale, 1997) using its variable time step feature. The realistic model of a hippocampal CA1 pyramidal neuron (Fig. 1A) was that used in a previous work (Migliore et al., 1999), and included sodium, DR- and A-type potassium (I_{Na}, I_{KDR}, and I_{A}, respectively) currents. In general, all conductances were based on the available experimental data for CA1 neurons (reviewed in Migliore and Shepherd, 2002). Briefly, the I_{Na} and I_{KDR} were uniformly distributed, whereas the peak conductances for I_{A} was linearly increased with distance from the soma (Hoffman et al., 1997) up to 500 μm. A non-inactivating, non-specific cation current $I_h = g_h \cdot n \cdot (V - E_{\mathrm{rev}})$, with $E_{\mathrm{rev}} = -30$ mV was also included in the soma and the apical dendrites. Its dendritic distribution and activation kinetics (Fig. 1B) were consistent with the available experimental data on CA1 neurons (Magee, 1998; Poolos et al., 2002). The activation curve was shifted by -8 mV in compartments >100 μm from soma, with a peak conductance density of $g_h = 0.5\ \mathrm{pS}/\mu\mathrm{m}^2$ at the soma, linearly increasing with distance, d (μm), as $g_{\mathrm{h}} \cdot (1 + 3d/100)$.

This model has already been shown to be in good agreement with a number of experimental results on the role of I_A on AP backpropagation (Migliore et al., 1999), on spike-timing dependent synaptic plasticity (Watanabe et al., 2002), and on the effects of pharmacological upregulation of I_h (Poolos et al., 2002).

Except where otherwise noted, only excitatory AMPA conductances were used to model synaptic inputs. They were implemented using a double exponential function (the Exp2Syn() built-in function of NEURON), the experimentally observed values of 0.5 and 3 ms for the rise and decay time, respectively (Andrasfalvy and Magee, 2001), and a reversal potential of 0 mV. Several synapses were activated in different dendritic regions (0–50 μm, 125–175 μm, 225–275 μm, and 325–375 μm), to explore neuronal excitability for synaptic inputs activated at different distances from soma. The number of synapses and the peak conductances, g_{syn}, used for each region are indicated in the figure legends. In a specific set of simulations, a NMDA conductance was also included in the synapses. It was implemented with a custom modification of a minimal kinetic scheme (to adapt the format to the event driven scheme used in the latest versions of NEURON) originally based on a NEURON model (Destexhe et al., 1994) fitting experimental data (Jahr and Stevens, 1990, 1990b). Following experimental suggestions (Andrasfalvy and Magee, 2001), the same (constant) peak conductance $g_{\mathrm{NMDA}} \cong 0.4 \cdot g_{\mathrm{syn(soma)}}$ was used for all synapses. An external magnesium concentration of 1 mM and a reversal potential of 0 mV were assumed.

In most cases, 75 synapses were used for all regions and, in order to compare the results for different regions, g_{syn} was scaled with distance from soma in such a way to obtain a somatic spike in all cases under synchronized synaptic activation, and roughly the same, high ($\sim$75–90%), spike probability during random synaptic activations in the absence of I_h. In this way we compensated for location-dependent effects due to all the other mechanisms, isolating the effects caused by I_h. The final values used in each region (0.5–2.6 nS) turned out to be consistent with a number of experimental findings suggesting an increase of synaptic conductance with distance from soma (Stricker et al., 1996; Magee and Cook, 2000; Andrasfalvy and Magee, 2001), and in quantitative agreement with experimental findings (Magee and Cook, 2000) suggesting a location-independent somatic EPSP amplitude (data not shown). Different combinations of g_{syn}, time constants, number of synapses, and spatial distributions were tested in preliminary simulations with no qualitative differences in the results.

The spike probability was obtained by testing for the presence of an action potential in 200 ms long simulations in which the synapses were activated, on

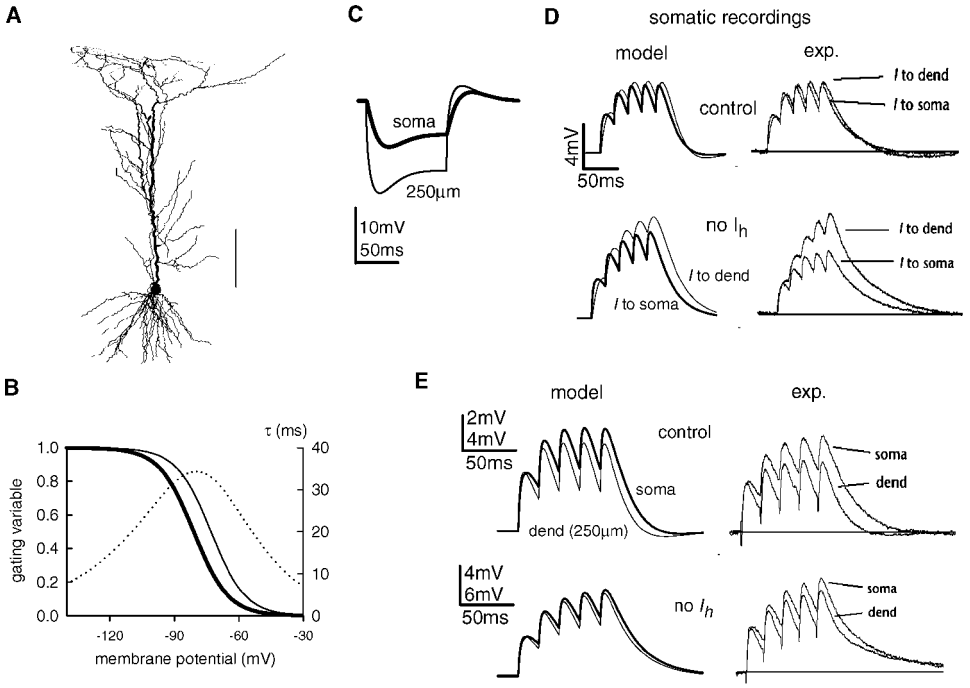

Figure 1. Effects of dendritic I_h on the temporal summation of EPSPs. A: The model neuron used in the simulations (calibration bar: 100 μm). B: Voltage-dependence of the steady-state (*solid lines*) and time constant (*dotted line*) of g_h activation for proximal (*light line*, soma and dendrites $<$100 μm) or distal (*heavy line*, $>$100 μm) compartments. C: Membrane potential at the soma and at a distal dendritic location (250 μm) during a dendritic current injection ($-$0.3 nA, 100 ms). D: Somatic depolarization, produced by a train of 5 EPSCs at 50 Hz injected in the soma (*heavy lines,* $I_{\text{peak}} = 0.1$ nA) or at 250 μm (*light lines*, $I_{\text{peak}} = 0.2$ nA), under control conditions (*top*) or without I_h (*bottom*). E: Local depolarization produced by a train of 5 EPSCs at 50 Hz injected in a distal dendrite (*light lines*) or in the soma (*heavy lines*) under control conditions (*top traces*) and without I_h (*bottom traces*). Experimental traces reproduced, with permission, from Figs. 2 and 4 of Magee (1999).

average, after 100 ms. For each dendritic region, 100 simulations were carried out randomly redistributing the synaptic locations (within the same region) in each simulation. To model different amounts of synchronization in the activation times, an adjustable parameter (a standard feature of the built-in *NetStim* class of NEURON) was used to set a "noise fraction", to activate each synapse at a more or less random (poissonian) times. The interstimuli intervals, T_{ISI}, were thus calculated as $T_{\text{ISI}} = (1 - nfrac)\cdot\nu + nfrac\cdot\text{P}(\nu)$, where *nfrac* is the noise fraction, ν the average T_{ISI} (100 ms, in our case), and P(ν) a random number drawn from a Poissonian distribution with a mean ν. By changing *nfrac* from 0 (corresponding to a synchronous activation of all synapses) to 1 (corresponding to a random synaptic activation), we were thus able to obtain different degrees of synchronization in the activation times. The NEURON models and simulation files are publicly available under the ModelDB section of the Senselab database (http://senselab.yale.med.edu).

Results

Validation of the Model

The typical experimental findings on the effects of a dendritic I_h in CA1 (Magee, 1998, 1999) and neocortical (Williams and Stuart, 2000) pyramidal neurons are: (i) a characteristic sag observed in the membrane potential during a hyperpolarizing current injection; (ii) the removal of location-dependent variability in temporal integration at the soma; and (iii) the generation of a spatial gradient for the local temporal summation. We further validated our model by reproducing all of these effects in the simulations. It should be stressed that, since we were interested in showing that the model was able to capture the most important effects of I_h, rather than model a particular neuron under particular experimental conditions, no attempt was made to fit experimental traces. The simulation findings are shown in Fig. 1C–E. To isolate the effect of I_h, we modeled the

experimental application of the channel blockers TTX, TEA and 4-AP in the bath by excluding, for these simulations, I_{Na}, I_{KDR}, and I_A from the model. To show the sag in both dendritic and somatic membrane potential, a hyperpolarizing current (−0.3 nA, 100 ms) was injected in a distal compartment ∼250 μm from the soma (Fig. 1C). To demonstrate that a dendritic I_h results in location-independent temporal integration at the soma, we show in Fig. 1D somatic traces during a 50 Hz train of current injections (time constants of 0.4 and 10 ms for rise and decay time, respectively) activated either at the soma (Fig. 1D, heavy lines) or at a distal compartment (Fig. 1D, light lines), with (Fig. 1D, top) or without (Fig. 1D, bottom) I_h. Finally, to illustrate that I_h generates a nonuniform local temporal summation, somatic and dendritic traces are shown in Fig. 1E with (Fig. 1E, top) or without (Fig. 1E, bottom) I_h from simulations of EPSCs activated at the soma or in a dendritic compartment at ∼250 μm. These results demonstrated that our model was able to reproduce the most significant experimental observations on the effects of a dendritic I_h in CA1 neurons.

I_h Selectively Reduces Neuronal Excitability for Unsynchronized Distal Inputs

Validation of the model against these experimental findings allowed us to make, with reasonable confidence, predictions on new effects that have not yet been explored experimentally. We were interested in elucidating the detailed role of the mechanisms involved in the integration of synaptic inputs that may lead to an AP. This is a significant event for CA1 neurons, which fire (on average) at a low rate (Csicsvari et al., 1999). Here we investigated the effects of dendritic I_h on neuronal excitability for strong synaptic inputs, to test our hypothesis that the I_h-dependent reduction in the temporal summation of synaptic inputs should differentially affect unsynchronized inputs, with respect to synchronized ones. Furthermore, since in CA1 and neocortical pyramidal neurons the I_h density increases with distance from soma, this effect should also depend on the dendritic location of the synaptic inputs.

The main effect is illustrated in Fig. 2, where we show superpositions of ten typical recordings from simulations of random synaptic activation (i.e. *nfrac* = 1) in proximal or distal dendritic compartments, with or without I_h. Without I_h, both proximal and distal random synaptic activations produced a somatic spike with the same (high) probability. The presence of I_h did not produce major changes in the spike probability for a proximal stimulation (Fig. 2, top, compare left and right traces), whereas it was drastically reduced for activation of distal inputs (Fig. 2, middle), even if their synchronous activation would always produce a somatic spike (data not shown). Consistently with experimental observations using strong local EPSCs injections (Magee, 1999), in many cases dendritic stimulation (Fig. 2, bottom) resulted in local initiation of dendritic spikes that did not propagate as action potentials to the soma. Simulation findings for different dendritic locations as a function of noise fraction are summarized in Fig. 3. In all cases, approximately the same spike probability (∼75–90%) was obtained for unsynchronized inputs (noise fraction = 1) in the absence of I_h (Fig. 3, open symbols). Proximal inputs (<50 μm, Fig. 3, triangles up) still elicit a somatic spike with high probability (∼70%) even for unsynchronized inputs, whereas for more distal inputs the spike probability quickly decreases with synchronization, being only ∼5% for unsynchronized inputs beyond 300 μm.

The previous findings demonstrated that a dendritic I_h may reduce a neuron's excitability selectively for asynchronous distal inputs. This is a somewhat surprising finding. In fact, we are confronted with the counter-intuitive result of a location-dependent temporal summation when both the model (Fig. 1D) and experiments (Magee, 1999) suggested that the increase in I_h with distance from soma should remove this effect at the soma. There is, however, another effect that needs to be considered to explain how this could happen: the frequency dependence of the local (dendritic) temporal summation. In fact, although the increasing I_h density with distance normalizes temporal summation at the soma, it also drastically affects the local summation (Magee, 1999) in a frequency-dependent way, altering the spike probability. A demonstration of the consequences of this effect is shown in Fig. 4. In these simulations, 50 synapses at 0–50 μm and 325–375 μm from soma were sequentially activated once at a constant interval, to study the spike probability with inputs at constant frequency. The peak conductances were scaled in such a way to obtain roughly the same spike probability as function of the frequency in the absence of I_h (Fig. 4, open symbols), and 50 simulations were carried out for each frequency randomly repositioning the synapses within a given region. The presence of I_h (Fig. 4, closed symbols) resulted in a much larger effect for distal inputs, with a marked

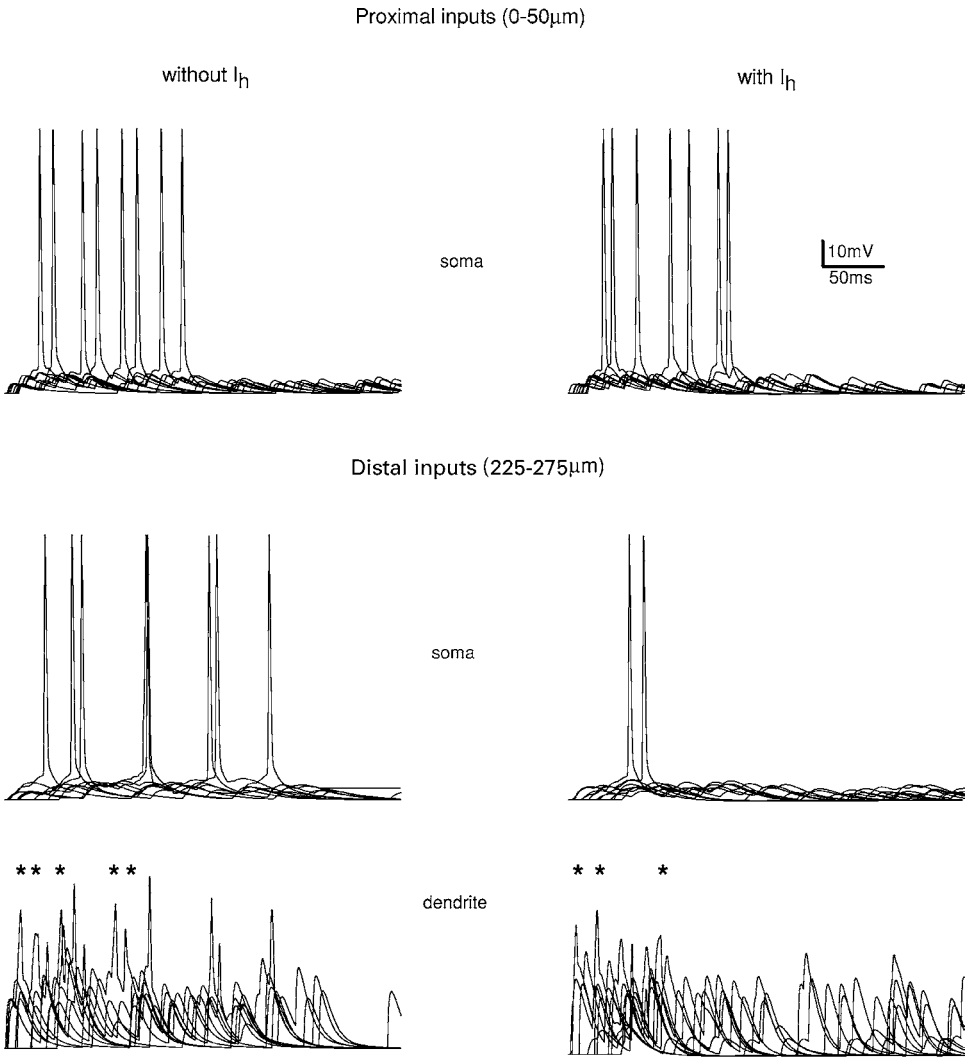

Figure 2. A dendritic I_h reduces a neuron's excitability during unsynchronized distal synaptic inputs. Each panel shows a superposition of 10 simulations. In each simulation, synaptic inputs to a proximal (*top panels*) or a distal (*middle and bottom panels*) dendritic region were randomly activated (*nfrac* $= 1$) in the absence (*left panels*) or with (*right panels*) I_h; $g_{\text{syn}} = 2.3$ nS ($n = 12$) and $g_{\text{syn}} = 10$ nS ($n = 12$) for proximal and distal synapes, respectively. Simultaneous somatic and dendritic (260 μm) recordings are shown for distal stimulation. Symbols in bottom traces indicate local dendritic spikes that did not propagate to the soma.

suppression of spikes for a larger frequency range, with respect to proximal ones. The inclusion of a NMDA conductance, using the experimentally suggested distribution of NMDA receptors (Magee, 1999), resulted in an additional difference in the effects of I_h for distal dendrites (Fig. 4, compare closed circles and squares). These effects also depended on the synaptic conductances, with a smaller number of larger synapses resulting in a larger difference between proximal and distal inputs (data not shown). These results explains why asynchronous inputs, which have a wider distribution of interstimulus intervals, might result in a much lower spike probability than synchronized inputs, which correspond to high frequency stimulation.

Different dendritic density, distribution, time constants, and voltage dependence, are found for I_h in different neurons, and activity-dependent (Luthi and McCormick, 1999), developmental (Vasilyev and Barish, 2002), or pathologic (Chen et al., 2001) changes may independently modulate them. We thus studied how different I_h properties may affect the spike probability. A series of simulations was carried out,

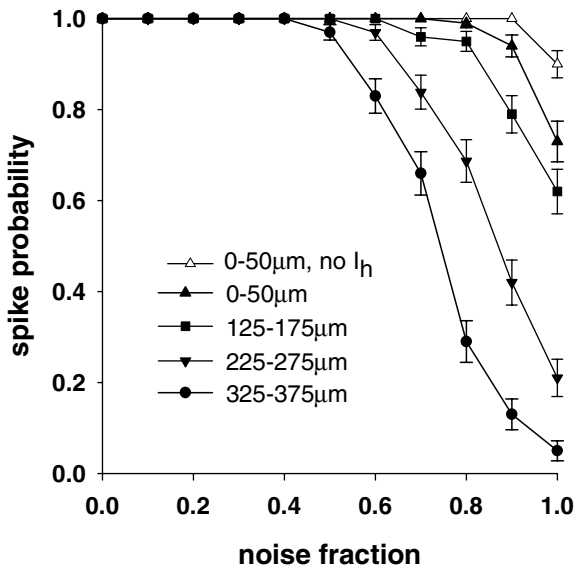

Figure 3. Spike probability as a function of noise fraction in the activation time of synapses at different distances from soma. Open symbols represent spike probabilities in the absence of I_h; the g_{syn} for the synapses at different distances from soma were: 0.5 nS (0–50 μm), 0.9 nS (125–175 μm), 1.6 nS (at 225–275 μm), and 2.6 nS (325–375 μm); 75 synapses were used in all cases; average and s.e.m calculated from 100 simulations.

increasing the density, the time constant, or shifting by +10 mv its activation curve, and the results are shown in Fig. 5. The simulation findings are better appreciated by comparing the results for control (Fig. 3) with those obtained for the same region under different conditions (Fig. 5). With respect to control, the spike probability in the most proximal region (Fig. 5, upper left) was relatively little affected by a 3-fold increase in density or in the time constant, or by a shift in the activation curve, and the spike probability was >40% in all cases for random inputs (noise fraction = 1). More distal regions, instead, were mostly affected by a density increase and by a shift in the activation curve, while they were not significantly affected by a 3-fold increase in the time constant (Fig. 5, compare black circles and triangles down).

Discussion

With a realistic model of a CA1 neuron, this study has demonstrated an experimentally testable effect of the dendritic I_h on neuronal excitability. It was previously shown (Poolos et al., 2002) that pharmacological modulation of I_h in CA1 hippocampal neurons could be used to selectively control dendritic excitability and epileptogenesis. Here, we have shown that the physiological dendritic distribution of I_h has a major role in selectively regulating synaptic integration of unsynchronized inputs on distal dendrites (Figs. 2 and 3). Our model predicts that, because of its frequency-dependent effects on the local dendritic summation of synaptic inputs (Fig. 4), the I_h would filter out a volley of strong distal excitatory afferents when they are

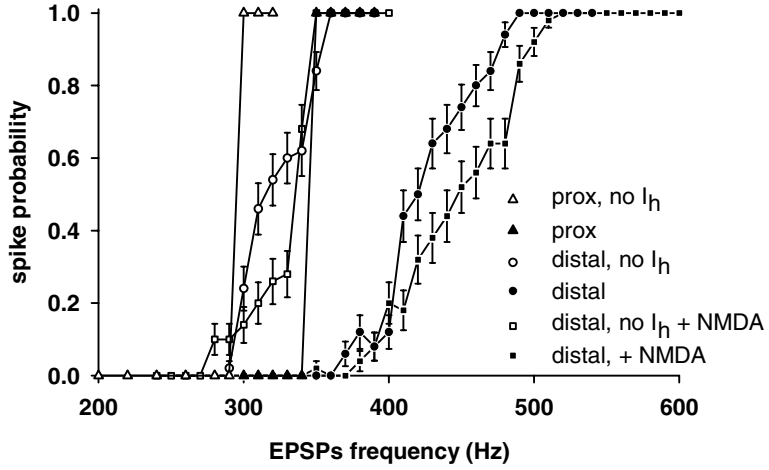

Figure 4. Spike probability during a sequential activation, at different constant frequencies, of synapses randomly located within a proximal or distal dendritic region with (closed symbols) or without (open symbols) I_h. 50 synapses were used in all cases. For simulations with AMPA (triangles and circles), $g_{\text{syn}} = 0.7$ nS and 1.8 nS for proximal and distal stimulations, respectively. For simulations with AMPA + NMDA (squares), $g_{\text{syn}} = 1.2$ nS and $g_{\text{NMDA}} = 0.3$ nS.

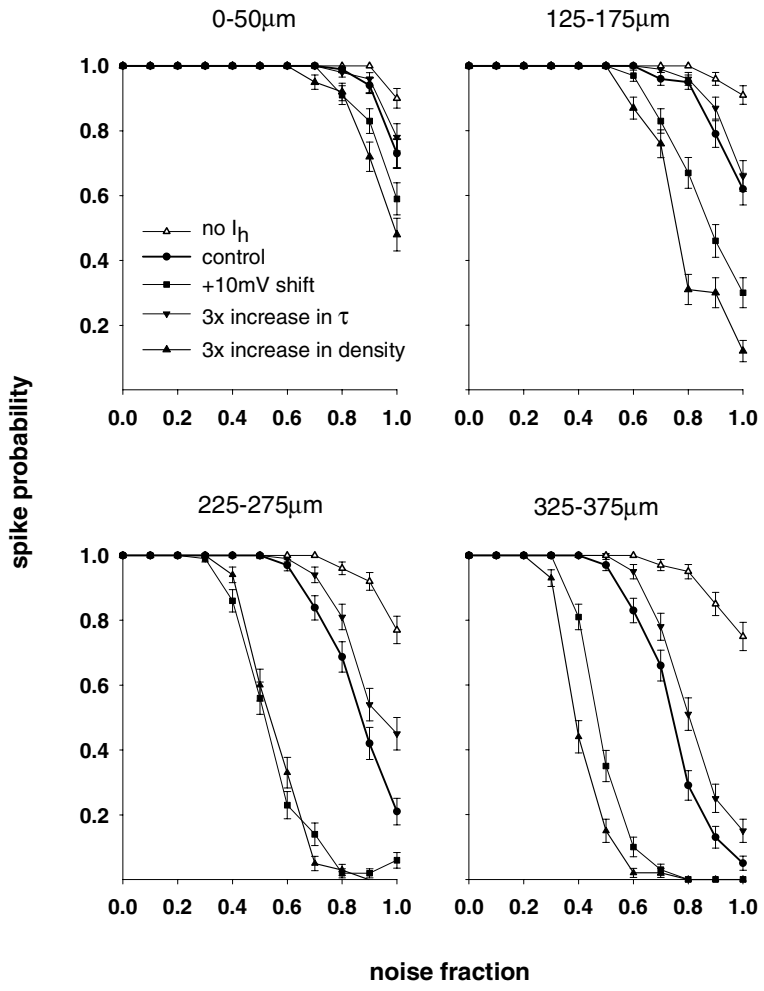

Figure 5. Effects of different I_h density or kinetic properties. Spike probability as a function of noise fraction at different distances from soma for a 3-fold increase in g_h (closed triangles up), a 3-fold increase in the time constant of activation (triangles down), or a +10 mV shift of the activation curve (squares).

asynchronously activated. The overall emerging picture is one in which proximal inputs would be unaffected in their ability to elicit a somatic action potential, independently of their relative synchronization, while the temporal summation of distal inputs will be progressively reduced as they desynchronize, in such a way to prevent AP generation in most cases when they are independently activated. As suggested by the findings illustrated in Fig. 5, the overall amount of this effect in any given neuron could be dynamically modulated, since it depends on kinetic properties (such as peak current and kinetics) that may change during development (Brewster et al., 2002) or with neuronal activity (Vargas and Lucero, 2002). Of course, many other dendritic mechanisms may affect the overall results. And thus, Ca^{++} currents, persistent Na^{+} or Ca-dependent K^{+} currents, activity-dependent changes in channels density of kinetic, non-uniform distribution of the various Ca^{++} currents, intracellular Ca^{++} dynamics, etc., may independently modulate the temporal summation of synaptic inputs. After the predictions of our model have also been experimentally confirmed, it would then be interesting to investigate how and to what extent they contribute to the differential temporal summation of unsynchronized proximal or distal inputs.

What functional relevance could such an effect have? It should be noted that the main hippocampal afferent pathways on CA1 neurons, the Schaffer collaterals and the perforant path, target the proximal and distal dendritic regions, respectively, and there might be precise

temporal requirements for their integration at the soma (Migliore, 2003). In addition to targeting different portions of the dendritic tree, these pathways might also be expected to have distinctly different activity patterns. In fact, the Schaffer collaterals originate from the CA3 hippocampal neurons, which are (mainly) bursting cells (Suzuki and Smith, 1985; Bilkey and Schwartzkroin, 1990), whereas the perforant path fibers originate from cells of the superficial layers of the enthorhinal cortex (Johnston and Amaral, 1998), which are regularly firing neurons (Dickson et al., 1997). Even if the firing of CA3 neurons may be modulated and synchronized by gamma oscillations (Traub et al., 1996), the synaptic activity caused by the Schaffer collaterals on a CA1 neuron would still be most likely unsynchronized, because of the intrinsic variability in bursting properties of CA3 cells (Suzuki and Smith, 1985). The regular firing of ECIII neurons, which also discharge in phase with gamma (Chrobak and Buzsáki, 1998) and theta (Frank et al., 2001) rhythms, would instead most likely result in a synchronized synaptic activity on the distal dendrites of a CA1 neuron. Given the current strong consensus on the importance of synchronized signals in brain function, a decrease in the synchronization of a population of synaptic inputs that are otherwise synchronized may be considered as the result of a change (e.g. in behavioral state or in the phase precession within the population) that might be necessary to exclude from the temporal integration of the inputs occurring within a given neuron. A mechanism is then needed to control this process. Our model suggests that a dendritic I_h, with dynamically modulated kinetic properties specifically tailored to act on EPSPs, rather than on action potentials (such as fast K^+ currents) or statically on all signals (such as a leakage current), might be such a mechanism.

Acknowledgments

We thank Ted Carnevale, Gordon Shepherd, Michael Hines, Wei Chen, and Tom Morse for useful comments and discussions. Support from NIDCD (Human Brain project) is acknowledged.

References

Andrasfalvy BK, Magee JC (2001) Distance-dependent increase in AMPA receptor number in the dendrites of adult hippocampal CA1 pyramidal neurons. J. Neurosci. 21: 9151–9159.

Bilkey DK, Schwartzkroin PA (1990) Variation in electrophysiology and morphology of hippocampal CA3 pyramidal cells. Brain Res. 514: 77–83.

Brewster A, Bender RA, Chen Y, Dube C, Eghbal-Ahmadi M, Baram TZ (2002) Developmental febrile seizures modulate hippocampal gene expression of hyperpolarization-activated channels in an isoform- and cell-specific manner. J. Neurosci. 22: 4591–4599.

Chen K, Aradi I, Thon N, Eghbal-Ahmadi M, Baram TZ, Soltesz I (2001) Persistently modified h-channels after complex febrile seizures convert the seizure-induced enhancement of inhibition to hyperexcitability. Nat. Med. 7: 331–337.

Chrobak JJ, Buzsáki G (1998) Gamma oscillations in the Entorhinal Cortex of the freely behaving rat. J. Neurosci. 18: 388–398.

Destexhe A, Mainen ZF, Sejnowski TJ (1994) An efficient method for computing synaptic conductances based on a kinetic model of receptor binding. Neural Comp. 6: 10–14.

Destexhe A, Pare D (1999) Impact of network activity on the integrative properties of neocortical pyramidal neurons in vivo. J. Neurophysiol. 81: 1531–1547.

Dickson CT, Mena AR, Alonso A (1997) Electroresponsiveness of medial entorhinal cortex layer III neurons in vitro. Neuroscience 81: 937–950.

Frank LM, Brown EN, Wilson MA (2001) A comparison of the firing properties of putative excitatory and inhibitory neurons from CA1 and the entorhinal cortex. J. Neurophysiol. 86: 2029–2040.

Hines M, Carnevale T (1997) The NEURON simulation environment. Neural Comp. 9: 178–1209.

Hoffman DA, Magee JC, Colbert CM, Johnston D (1997) K+ channel regulation of signal propagation in dendrites of hippocampal pyramidal neurons. Nature 387: 869–875.

Ho N, Destexhe A (2000) Synaptic background activity enhances the responsiveness of neocortical pyramidal neurons. J. Neurophysiol. 84: 1488–1496.

Jahr CE, Stevens CF (1990) A quantitative description of NMDA receptor-channel kinetic behavior. J. Neurosci. 10: 1830–1837.

Jahr CE, Stevens CF (1990b) Voltage dependence of NMDA-activated macroscopic conductances predicted by single-channel kinetics. J. Neurosci. 10: 3178–3182.

Johnston D, Amaral DG (1998) Hippocampus In: GM Shepherd, ed. The Synaptic Organization of the Brain, 4th ed. Oxford Univ. Press, New York, pp. 417–458.

Luthi A, McCormick DA (1999) Modulation of a pacemaker current through Ca(2+)-induced stimulation of cAMP production. Nat. Neurosci. 2: 634–641.

Magee JC (1998) Dendritic hyperpolarization-activated currents modify the integrative properties of hippocampal CA1 pyramidal neurons. J. Neurosci. 18: 7613–7624.

Magee JC (1999) Dendritic Ih normalizes temporal summation in hippocampal CA1 neurons. Nat Neurosci. 2: 508–514.

Magee JC, Cook E (2000) Somatic EPSP amplitude is independent of synapse location in hippocampal pyramidal neurons. Nature Neurosci. 3: 895–903.

Megias M, Emri Z, Freund TF, Gulyas AI (2001) Total number and distribution of inhibitory and excitatory synapses on hippocampal CA1 pyramidal cells. Neuroscience 102: 527–540.

Migliore M (2003) On the integration of subthreshold inputs from Perforant Path and Schaffer collaterals in hippocampal CA1 neurons. J. Comput. Neurosci. 14: 185–192.

Migliore M, Hoffman DA, Magee JC, Johnston D (1999) Role of an A-type K+ conductance in the back-propagation of action potentials in the dendrites of hippocampal pyramidal neurons. J. Comput. Neurosci. 7: 5–16.

Migliore M, Shepherd GM (2002) Emerging rules for the distributions of active dendritic conductances. Nature Rev. Neurosci. 3: 362–370.

Penny WD, Kiebel SJ, Kilner JM, Rugg MD (2002) Event-related brain dynamics. Trends Neurosci. 25: 387–389.

Poolos NP, Migliore M, Johnston D (2002) Pharmacological upregulation of h-channels selectively reduces the excitability of pyramidal neuron dendrites. Nature Neurosci. 5: 767–774.

Spruston N, Schiller Y, Stuart G, Sakmann B (1995) Activity-dependent action potential invasion and calcium influx into hippocampal CA1 dendrites. Science 268: 297–300.

Stricker C, Field AC, Redman SJ (1996) Statistical analysis of amplitude fluctuations in EPSCs evoked in rat CA1 pyramidal neurones in vitro. J. Physiol. 490: 419–441.

Suzuki SS, Smith GK (1985) Burst characteristics of hippocampal complex spike cells in the awake rat. Exp. Neurol. 89: 90–95.

Traub RD, Whittington MA, Colling SB, Buzsaki G, Jefferys JG (1996) Analysis of gamma rhythms in the rat hippocampus in vitro and in vivo. J. Physiol. 493: 471–484.

Vargas G, Lucero MT (2002) Modulation by PKA of the hyperpolarization-activated current (I_h) in cultured rat olfactory receptor neurons. J. Membr. Biol. 188: 115–125.

Vasilyev DV, Barish ME (2002) Postnatal development of the hyperpolarization-activated excitatory current I_h in mouse hippocampal pyramidal neurons. J. Neurosci. 22: 8992–9004.

Watanabe S, Hoffman DA, Migliore M, Johnston D (2002) Dendritic K^+ channels contribute to spike-timing dependent long-term potentiation in hippocampal pyramidal neurons. Proc. Natl. Acad. Sci. USA 99: 8366–8371.

Williams SR, Stuart GJ (2000) Site independence of EPSP time course is mediated by dendritic $I(h)$ in neocortical pyramidal neurons. J Neurophysiol 83: 3177–3182.